2024 IEEE International Conference on Robotics and Automation (ICRA 2024)
May 13-17, 2024. Yokohama, Japan

The Fractal Hand–I: A Non-anthropomorphic, but Synergistic, Adaptable Gripper

Joel W. Burdick and Malcolm Tisdale

***Abstract*— We introduce a novel *Fractal Hand* robotic gripper. The hand has only 1 actuator, but $(2^{n+1}-1)$ joints, where a design parameter n defines the depth of the fingers' tree structures. The hand is *synergistic* in its operation (because its joint movements are coupled through the hand's interaction with the grasped object), but it is not anthropomorphic. The basic finger and hand geometry, governing kinematics, and quasi-statics mechanics of a rigid version of the hand are developed. These analyses remarkably show that under mild constraints, the grasped object is compliantly stable at an equilibrium grasp configuration. Thus, the Fractal Hand adapts to a very wide range of planar objects with a single design. Grasp planning is thus simplified. A companion paper [33] introduces a design methodology for this new class of robot hands, and multiple prototypes.**

I. Introduction

Mechanical hands are an essential tool for robotic acquisition and manipulation of objects. Significant effort has gone into the design [6] and analysis of robotic hands [24], as well as the algorithms needed to plan and control their deployment [13], [14], [19]. While existing hand designs are quite varied, many robotic hands use an anthropomorphic design architecture based on multiple independent serial-chain finger mechanisms attached to a common palm. Each mechanism joint is actuated, leading to potentially complex and expensive designs, and complicated planning and control algorithms. Moreover, accurate control of these devices during manipulation can require complex sensing devices [34] and sensor data interpretation algorithms.

Because highly reliable and robust execution of multi-fingered grasps on novel objects continues to be a challenge, a variety of research and development efforts have aimed to create mechanically simpler hands with fewer actuators. While the use of fewer actuators may limit the complexity of achievable grasps, this limitation can often be balanced by a reduction in cost and mechanical complexity, and an increase in the robustness of workpiece acquisition. Progress in soft mechanism design and manufacturing techniques has opened up the space of possible robot hand designs [1], [4], including nonanthropomorphic origami based fingers or grippers [12]. However, their lower precision and lower achievable grasping forces limit the application of soft gripping devices.

The use of *synergies* [2] in the design and control of multi-fingered hands has been a fruitful approach. Synergistic designs often use two principles. First, reaction wrenches on the hand, generated by contact with the environment, can provide a passive form of grasp control and adaptation [5], [6], [29]. Second, coupling of joint movements can further shape the hand's response [23], [25]. While joint couplings can be performed by computer, mechanical couplings further the goal of reducing the actuator count [18], [25].

Dept. of Mechanical and Civil Engineering, California Institute of Technology, Mail Code 104-44, Pasadena, CA 91125. *jburdick@caltech.edu*

Fig. 1: Picture of a Fractal Vise taken from [32]

This paper introduces a novel *Fractal Finger* and a *Fractal Hand* for robotic grasping. While the hand is constructed with $(2^{n+1}-1)$ joints, where n is a design parameter, it requires only one actuator to operate. The remaining degrees of freedom operate in a coupled, or synergistic, manner, but its coupling is very different than previous synergistic hand designs, and its design is not anthorpomorphic. Moreover, its synergy is nearly universal, in that its mechanical adaptation process is largely independent of the object shape.

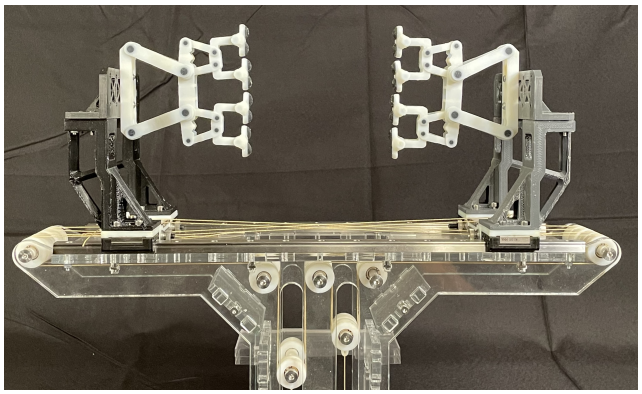

Fig. 2: Picture of a Fractal Hand prototype. Two fractal fingers are mounted to a prismatic closing actuator. The Remote Center quadrilaterals in this prototype replace the the Fractal Vise's sliding dovetail revolute joints. See [33] for details, and additional prototypes.

The fractal finger and fractal hand designs are inspired by a novel *fractal* mechanical vise (e.g, see Fig. 1) that was

patented in 1913 [10], and manufactured in the 1920's by the Mantle Co. [20], [32]. Empirically, this vise can stably and firmly hold virtually any planar object, even though it is not actuated (other than its closing power screw). This paper not only adapts this concept to robotic grasping, but presents a first attempt at understanding the working principles behind this mechanism. A companion paper [33] introduces new design ideas for fractal hands that overcome some of the limitations of the original fractal vise design, and establishes principles for future work in this area.

The joints of each *fractal finger* form a tree topology. Previousstudies of tree topology mechanisms [8], [15], [16], [28] have focused on dimensional synthesis for specific tasks or specific tree-topology hands [7], [9], [27], [30]. Whipple tree mechanisms, tree structured devices that balance loads across the tree, have also been used in hand design [31]. The fractal hand has a larger and more adaptable workspace than these devices. Moreover, this paper studies tree mechanisms of arbitrary depth, and develops some of their properties that have not been previously investigated.

We show that nearly every fractal hand equilibrium grasp of a planar object with locally smooth boundaries is compliantly stable. These results imply that grasp planning with fractal hands should be easy.

This paper focuses on binary tree topologies, but other topologies are possible. Many of this paper's concepts also extend to 3-D hands. Section II introduces the descriptive geometry of fractal fingers and hands. After Section III summarizes their basic kinematic properties, Section IV investigates the properties of rigid body fractal hand models, showing that their adaptivity does not arise from classical first-order rigid body effects. Section V shows that every fractal hand equilibrium grasp is second-order immobile under mild conditions, and therefore every equilibrium grasp is a secure grasp. The companion paper [33] introduces principles for Fractal Hand design, fractal hand prototypes, and grasping demonstrations.

II. The Rigid Fractal Hand: Description, Geometry, and Nomenclature

A. Fractal Finger Description and Nomenclature

A planar fractal finger consists of rigid links connected by revolute joints arranged in a binary *joint tree* (see Fig. 4). The *base joint* forms the tree's root node. An n-*level fractal finger* includes $(n-1)$ levels of children joints below the base joint. The edges in the tree correspond to rigid links.

An n-level fractal finger possesses (2^n-1) revolute joints whose joint axes and rotational angles are indexed as follows. The base joint angle and joint axes are respectively denoted θ_1 and $\mathcal{J}_1$. The joints and rotational angles of the children joints have two subscripts: $i \in \{2,\ldots,n\}$ indicates the *level* of the joint in the joint tree, while $j \in \{1,\ldots,2^{i-1}\}$ sequentially indexes the joints across the level. E.g., $\theta_{2,1}$ is the angle of the 1^{st} joint, $\mathcal{J}_{2,1}$, in the second tree level. The vector of fractal finger joint angles is organized by levels:

$$\vec{\theta} = \left[\theta_1;\, \theta_{2,1}\, \theta_{2,2};\, \theta_{3,1} \cdots \theta_{3,4};\, \cdots;\, \theta_{n,1} \cdots \theta_{n,(2^n-1)}\right]^T.$$

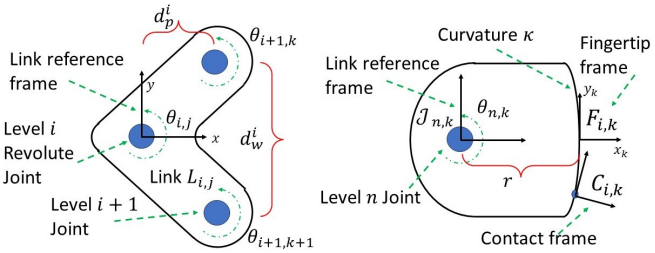

Fig. 3: **Left:** Geometry of a fractal finger link. **Right:** geometry of a fingertip link.

An i^{th}-level (for $i = 1,\ldots,n-1$) *finger link*, $L_{i,j}$, connects to a level-$(i-1)$ *parent* finger link through a single revolute joint at joint level i, and connects to its two *children* links via revolute joints at joint level $(i+1)$. Links in the same level are sequentially indexed via subscript j. The base joint connects to a base link, which forms part of the fractal hand, as described below (see Fig. 4). A finger *base frame*, B_i for $i \in \{1,2\}$, is attached to the base of each finger. For notational convenience, a *palm frame*, $\mathcal{P}$, is chosen to be coincident with B_1. The grasped object's configuration, $q \in SE(2)$, is defined by the pose of $\mathcal{O}$ relative to $\mathcal{P}$.

Remark: This paper assumes that a single point contact between the object and each fractal finger-tip. This assumption implies that the relative curvature of the fingertip link and the object at the contact is positive. The original fractal vise, and our 3D-printed remote-center fractal finger prototype [33] actually contact the object at two points per finger link (e.g., see Fig. 1), which are symmetrically distributed on either side of the finger link's line of symmetry. While the advantages of the two point contact design are under investigation, this geometry better allows fractal fingertips to interface with locally convex or concave object surfaces.

The parent and children joints form an isosceles triangle (Fig. 3). The origin of each link's body fixed reference frame coincides with the parent joint axis, and its x-axis bisects the children joints. All links at the same level have uniform dimensions, which are defined as (Fig. 3):

- The *finger link width*, d_w^i for $i = 1,\ldots,(n-1)$, is the distance between the children joint axes at joint level i.
- The *link pitch*, d_p^i for $(i = 1,\ldots,n-1)$, equals the height of an i^{th}-level links' isosceles triangles.

Non-uniform dimensioning of links across a level is possible, and this issue is currently a subject of study. Rotary springs may be installed in some or all joints, as shown in the companion paper [33]. Such compliance enables the fingers to return to the pre-grasped shape.

The distal *fingertip links* connect to their parent links by an n^{th}-level revolute joint (see Fig. 3). Reference frame, F_k, (which may differ from a *contact frame*) is placed centrally at the fingertip. The distance from joint $\mathcal{J}_{n,k}$ to the origin of F_k is r, and the all contacting surfaces have curvature κ.

B. The Fractal Hand

A planar fractal hand consistsof two (or more) fractal fingers, connected by a single closing actuator, like a parallel

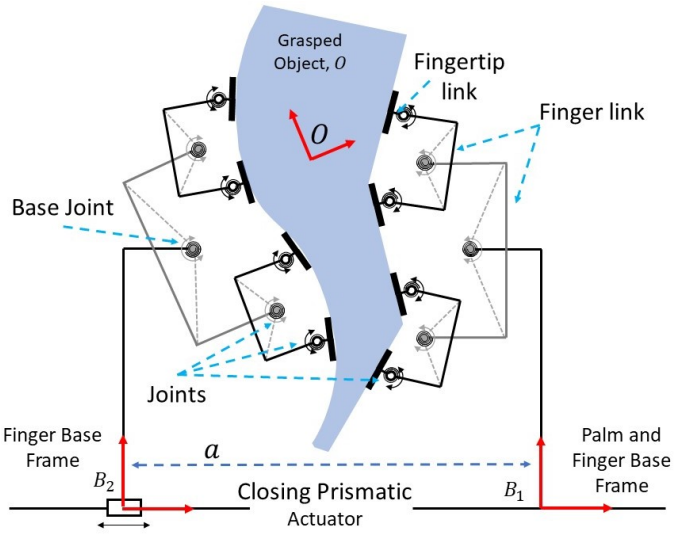

Fig. 4: Conceptual Geometry of a two-fingered fractal hand with tree depth $n = 3$, but n can be arbitrarily large.

jaw gripper. A single actuator adjusts the spacing between the two finger base frames. We model this movement by a prismatic joint, but it can be implemented in many ways. The composite vector of joint angles is denoted

$$\Theta = (\theta_1 \ \theta_2 \ a)^T \tag{1}$$

where a is the closing actuator distance (Fig. 4).

III. Rigid Fractal Finger/Hand Kinematics

This section summarizes basic kinematic quantities of relevance to the study of fractal fingers/hands.

A. The Fractal Finger Jacobian

An n-level fractal finger possesses 2^{n-1} fingertip links. Let $V_k = (x_{i,k} \ y_{i,k} \ \dot{\phi}_{i,k})^T$, $k = 1, \ldots, 2^{n-1}$, denote the rigid body velocity of the k^{th} fingertip frame, F_k, as described in B_i. The i^{th} finger's *Fractal Finger Jacobian*, $J_{F,i}(\theta_i)$, maps the mechanism's $(2^n - 1)$ joint velocities to the 2^{n-1} triads of fingertip frame velocities. Let $\vec{\xi}_{i,j}$ denote the vector

$$\vec{\xi}_{i,j} = \begin{bmatrix} M\vec{s}_{ij,k} \\ 1 \end{bmatrix} \quad \text{with} \quad M = \begin{bmatrix} 0 & -1 \\ 1 & 0 \end{bmatrix} \tag{2}$$

where $\vec{s}_{ij,k}$ is the vector from $joint\mathcal{J}_{i,j}$ to the origin of F_k. The $(3\times 2^{n-1})\times(2^n-1)$ dimensional fractal finger Jacobian matrix (in hybrid velocity coordinates) has the form:

$$J_{F_i}(\theta_i) = \begin{bmatrix} \vec{\xi}_1 & \vec{\xi}_{2,1} & 0 & \vec{\xi}_{3,1} & 0 & 0 & 0 & \vec{\xi}_{4,1} & \cdots \\ \vec{\xi}_1 & \vec{\xi}_{2,1} & 0 & \vec{\xi}_{3,1} & 0 & 0 & 0 & 0 & \cdots \\ \vdots & \vdots & \vdots & \vdots & \vdots & \vdots & \vdots & \vdots & \cdots \\ \vec{\xi}_1 & \vec{\xi}_{2,1} & 0 & 0 & \vec{\xi}_{3,2} & 0 & 0 & 0 & \cdots \\ \vec{\xi}_1 & 0 & \vec{\xi}_{2,2} & 0 & 0 & \vec{\xi}_{3,3} & 0 & 0 & \cdots \\ \vec{\xi}_1 & 0 & \vec{\xi}_{2,2} & 0 & 0 & \vec{\xi}_{3,3} & 0 & 0 & \cdots \\ \vdots & \vdots & \vdots & \vdots & \vdots & \vdots & \vdots & \vdots & \cdots \\ \vec{\xi}_1 & 0 & \vec{\xi}_{2,2} & 0 & 0 & 0 & 0 & 0 & \cdots \end{bmatrix}. \tag{3}$$

The matrix J_F^T maps the 2^{n-1} fingertip frame wrenches to the $(2^n - 1)$ joint torques. It is important to note that none of the finger joints are actuated. Instead, the fractal hand must use other physical phenomena to securely grasp an object.

B. The Fractal Grasp Map and Hand Jacobian

We assume that each fractal fingertip contacts the grasped object, $\mathcal{O}$, at a single point. The origin of each fingertip's *contact frame*, $\mathcal{C}_{i,j}$, lies at the contact point, with its x-axis defined as the outward pointing unit normal vector to the finger surface (see Fig. 3). The corresponding contact frame on $\mathcal{O}$, denoted $\mathcal{C}_{i,j}^{\mathcal{O}}$, has its origin at the contact point, and its x-axis is the unit vector pointing outward from $\mathcal{O}$, and antiparallel to the x-axis of $\mathcal{C}_{i,j}$. Vector $\vec{c}_{i,j}(\theta_i)$ for the j^{th} fingertip of the i^{th} finger points from the origin of frame B_i to the origin of frame $\mathcal{C}_{i,j}$ Let $\vec{f}_{i,j}$ denote the contact forces between the j^{th} fingertip of the i^{th} finger ($i \in \{1, 2\}$) and $\mathcal{O}$. Let $W_{i,j}$ denote the *wrench basis* of the j^{th} fingertip contact model, which describes (in frame $\mathcal{C}_{i,j}$) the forces which can be supported at the contact between the fingertip and $\mathcal{O}$. $W_{i,j}$ respectively takes the forms

$$W_{i,j} = \begin{bmatrix} 0 \\ 1 \\ 0 \end{bmatrix}, \qquad W_{i,j} = \begin{bmatrix} 1 & 0 \\ 0 & 1 \\ 0 & 0 \end{bmatrix} \tag{4}$$

for frictionless point contact, and point contact with friction models. Let $\vec{f}_i$ denote the vector of all finger i contact forces:

$$\vec{f}_i = (\vec{f}_{i,1} \ \vec{f}_{i,1} \ \cdots \ \vec{f}_{i,2^{n-1}})^T. \tag{5}$$

The block-diagonal matrix $\tilde{W}_i$ organizes all of the i^{th} finger's contact models ($i = 1, 2$):

$$\tilde{W}_i = \begin{bmatrix} W_{i,1} & 0 & \cdots & 0 \\ 0 & W_{i,2} & \cdots & 0 \\ \vdots & \cdots & \ddots & \vdots \\ 0 & \cdots & 0 & W_{i,2^{n-1}} \end{bmatrix}. \tag{6}$$

Finally, let $\vec{f} \triangleq \begin{bmatrix} \vec{f}_1 \ \vec{f}_2 \end{bmatrix}$ denote the vector of all contact forces of all fractal hand fingertips.

1) Grasp Map: The 2-fingered fractal hand grasp map [17], [22] takes the form $G = \begin{bmatrix} G_1 \ G_2 \end{bmatrix}$, where:

$$G_i = \begin{bmatrix} (Ad^T_{g_{OC^{\mathcal{O}}_{i,1}}} W_{i,1}) \cdots (Ad^T_{g_{OC^{\mathcal{O}}_{i,2^{n-1}}}} W_{i,2^{n-1}}) \end{bmatrix} \tag{7}$$

for $i \in \{1, 2\}$. Matrix $Ad^T_{g_{OC^{\mathcal{O}}_{i,j}}}$ transforms contact wrenches in frame $\mathcal{C}_{i,j}^{\mathcal{O}}$ to object frame, O. Matrices G_1 and G_2 have dimensions $3 \times (p \times 2^{n-1})$, where $p \in \{1, 2\}$ is the number of independent contact forces in the planar contact model. When G is full rank, note that its null space respectively has dimension $(2^{n-1} - 3)$ or $(2^n - 3)$ for $p = 1$ or $p = 2$.

2) Fractal Hand Jacobian: The *Fractal Hand Jacobian*, $J_H(\Theta)$, relates the hand's joint velocities to the fingertips' velocities that can be transmitted to $\mathcal{O}$. It includes the

influence of the closing actuator.

$$J_H \;=\; \begin{bmatrix} ({\tilde{W}_1}^T T^1_{CB_1} J^{\mathcal{C}}_{F,1}) & 0 & 0 \\ 0 & (\tilde{W}_2^T T^2_{CB_2} J^{\mathcal{C}}_{F,2}) & (\dot{a}\tilde{W}_2^T T^2_{CB_2}\mathbb{X}) \end{bmatrix}$$

where $\tilde{W}_i$ the wrench basis matrix (6), $\mathbb{X}$ is a column vector of 2^{n-1} x-vectors, $(1\ 0\ 0)^T$, and $\dot{a}$ is the velocity of the closing actuator. Matrix $J^{\mathcal{C}}_{F,i}$, for $i = 1, 2$, is the i^{th} fractal finger's Jacobian matrix (3), modified so that the motions of the fingertip contact frames, rather than the fingertip frames, define the output velocities of the Jacobian mapping. Note, in most analyses carried out below (which focus on equilibrium grasp conditions), the contact frame $\mathcal{C}_{i,j}$ and the fingertip frame, $F_{i,j}$, are coincident. Let matrix $T^i_{B_i C_{i,j}}$ transform velocities in contact frame $\mathcal{C}_{i,j}$ to base frame, B^i. Matrix $T^i_{CB_i}$ transforms all 2^{n-1} contact frame velocities, as represented in frame B_i, to their representations in the respective contact frames:

$$T^i_{\mathcal{C}B_i} \;=\; \begin{bmatrix} (T^i_{B_i\mathcal{C}_{i,1}})^{-1} \\ \vdots \\ (T^i_{B_i\mathcal{C}_{1,2^n-1}})^{-1} \end{bmatrix}.$$

Matrix J_H has dimension $(p \cdot 2^n) \times (2^{n+1} - 1)$, where $p = 1$ (2) for a frictionless (frictional) contact model. In a generic hand configuration, J_H^T has no null space. We will see below that this null space is nonempty, and takes a special form, in equilibrium hand configurations.

IV. First-Order Mechanical Properties of the Rigid Fractal Hand in Equilibrium

Empirical observations of the Fractal Vise show that it can securely hold planar workpieces with a nearly unlimited variety of shapes. How does the fractal hand adapt to each shape, given that it has no sensors and a single closing actuator? This section analyzes the vise-like hand's properties from a 1^{st}-order rigid body point of view , and concludes that such an analysis cannot fully explain the vise's (or hand's) observable properties. The following sections show that the hand's function can be understood by higher order effects.

The remainder of this section assumes that a 2-fingered fractal hand holds object $\mathcal{O}$ in an equilibrium grasp at configuration (Θ_0, q_0)). Let $G(q_0)$ and $J_H(\Theta_0, q_0)$ respectively denote the equilibrium Grasp Map and Hand Jacobian.

A. First-order analysis in contact space

Recall that when a multi-fingered hand grasps an object, the space of finger contact forces can be categorized into four sets with different physical interpretations [3], [22]. This force decomposition still holds for fractal fingers and hands:

- **Structurally dependent contact forces**. These fingertip forces, U_{sd}, lie in the range space of $G^T(q_0)$, denoted by $\mathcal{R}(G^T(q_0))$, and in the null space of J_H^T, denoted by $\mathcal{N}\big(J_H^T(\Theta_0, q_0)\big)$:

$$U_{sd} \;=\; \mathcal{R}(G(q_0)) \cap \mathcal{N}(J_H^T(\Theta_0, q_0)).$$

That is, a wrench, $\mathbf{w}$, applied to $\mathcal{O}$ can be resisted by reaction forces generated from the hand's structure, and not actuator forces, when $\mathbf{w} = G\vec{f}$ for $\vec{f} \in U_{sd}$.

- **Actively Controlled Forces:** This set of fingertip forces, denoted U_{act}, is directly modulated by the hand's actuators and can actively counterbalance external wrenches applied to $\mathcal{O}$:

$$U_{act} = L_{\mathcal{R}(G^T)}\big[\mathcal{N}(J_H^T(\Theta_0, q_0))^{\perp}\big].$$

where $L_{V_1}\big[(V_2)\big]$ denoted the orthogonal projection of vector space V_2 onto the vector space V_1.

- **Active Internal forces:** These forces, denoted N_{act}, lie in $\mathcal{N}(G)$ and in the complement of $\mathcal{N}(J_H^T(\Theta_0, q_0))$:

$$N_{act} \;=\; L_{\mathcal{N}(G)}\big[\big(J_H^T(\Theta_0, q_0)\big)^{\perp}\big].$$

These "squeeze" forces can be actively modulated by the fractal hand's one closing actuator.

- **Preloading forces.** These forces, denoted N_{pre}, lie in both $\mathcal{N}(G(q_0))$ and $\mathcal{N}(J_H^T(\Theta_0, q_0)$:

$$N_{pre} \;=\; \mathcal{N}(G) \cap \mathcal{N}(J_H^T(\Theta_0, q_0)).$$

Because the fractal fingers possess no actuators, the fractal hand cannot generate *any* actively controlled contact forces. In contrast, such forces are crucial to the operation of multi-fingered anthropomorphic robotic hands, including synergistic ones. To analyze these forces, we must first consider the constraints imposed by an equilibrium grasp condition.

B. Equilibrium Grasp Conditions

In an equilibrium grasp of a fractal hand containing two n-level fingers, the fingertip contact forces, $\vec{f}^{eq}$, applied to $\mathcal{O}$ must result in a zero net wrench on $\mathcal{O}$: $G\vec{f}^{eq} = \vec{0}$. However, the equilibrium condition also constrains the mechanism's configuration. For simplicity, we analyze the case of frictionless contact–an analysis of the frictional case reaches similar conclusions. In all cases, the joints are assumed frictionless.

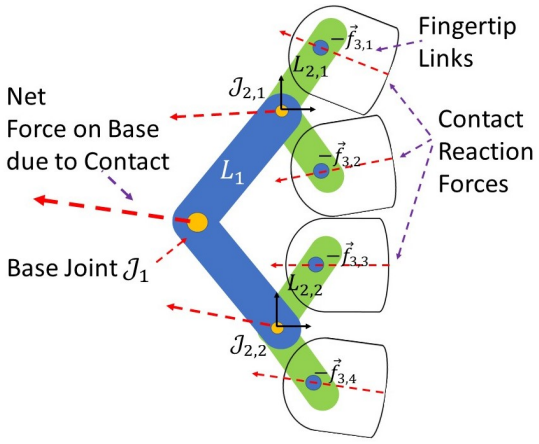

Fig. 5: Diagram of balanced torque condition

The line underlying the contact force applied to the j^{th} frictionless fingertip must pass through the axis of joint $\mathcal{J}_{n,j}$ (see Fig. 5), else there is an unbalanced torque about $\mathcal{J}_{n,j}$:

$$\tau_{n,j} = 0, \quad \forall j = 1, \cdot, 2^{(n-1)},$$

where $\tau_{n,j}$ denotes torque about $\mathcal{J}_{n,j}$ for either finger.

Next, consider two adjacent n^{th}-level fingertip links $L_{n,j}$ and $L_{n,j+1}$, that are joined to the same parent link (see Fig. 5). The lines underlying the contact force vectors $\vec{f}_{n,j}$ and $\vec{f}_{n,j+1}$ must each pass through the joint axes of their respective fingertip links. The contact forces magnitudes and their directions must result in a net zero torque *balancing condition* about the parent joint at level $(n-1)$:

$$\tau_{n-1,j} = (f_{n,j}cos(\theta_{n,j}) - f_{n,j+1}cos(\theta_{n,j+1}))d_w^{n-1}/2 - (f_{n,j}\sin(\theta_{n,j}) + f_{n,j+1}\sin(\theta_{n,j+1}))d_p^{n-1} = 0. \quad (8)$$

where $\theta_{n,j}$ is the angle of the j^{th} fingertip link (see Fig. 3). Under a frictionless contact, each level-n joint angle, $\theta_{n,j}$ for $j = 1, \ldots, 2^{n-1}$, is dictated by the tangent to the object boundary at the equilibrium contact. Hence, $\theta_{n,j}$ is determined for all $j = 1, \ldots, 2^{n-1}$ in the equilibrium grasp by the object shape and its pose within the hand. Thus Eq. (9) is only a function of the scalar forces $f_{n,j}$ and $f_{n,j+1}$.

Similar constraints must apply recursively to the parent joints, and ultimately to the base joint (see Fig. 5). If $\vec{\mathfrak{f}}_{i,j}$ denote the force passing through joint axis $\mathcal{J}_{i,j}$ when all of the descendent joints of joint $\mathcal{J}_{i,j}$ satisfy the torque balance condition, then for joint tree levels 1 to $n-1$, the following equation must be satisfied

$$\tau_{i-1,j} = (\mathfrak{f}_{i,j}cos(\theta_{i,j}) - \mathfrak{f}_{i,j+1}cos(\theta_{i,j+1}))d_w^{i-1}/2 - (f_{i,j}\sin(\theta_{i,j}) + f_{i,j+1}\sin(\theta_{i,j+1}))d_p^{i-1} = 0. \quad (9)$$

The torque balancing condition on the joints in levels 1 to $(n-1)$ provide $(2^{n-1}-1)$ scalar constraints on the set of 2^{n-1} fingertip normal contact forces. Note that if contact forces $\vec{f}^{eq}$ satisfy the torque balance constraints, then $\alpha\vec{f}^{eq}$ satisfies the constraint for all $\alpha \in (0, \infty)$. This torque balancing analysis proves the following two lemmas:

Lemma 1. *In a 2-fingered fractal hand equilibrium grasp involving frictionless contacts with the grasped object $\mathcal{O}$, $dim(\mathcal{N}(J_{F,i}^{\mathcal{C}})) = 1$ for $i \in \{1,2\}$, where $dim(V)$ is the dimension of vector space V,*

Lemma 2. *In an equilibrium grasp of a 2-fingered fractal hand, the range space of matrix $\tilde{W}_i^T$ lies in the null space of each finger Jacobian: $\mathcal{R}(\tilde{W}_i) \subseteq \mathcal{N}(J_{F,i}^{\mathcal{C}})$, for $i \in \{1,2\}$.*

The direction of the reaction force vector imposed on the base link at $\mathcal{J}_1$ (Fig. 5) by the fingertip contact forces depends upon the finger's equilibrium pose. The torque balance condition implies that its amplitude can vary by a positive scalar factor, α.

Since a single fractal finger can counterbalance a 1-dimensional set of contact forces, a 2-fingered hand can have at most a 2-dimensional null space for its hand Jacobian: $dim(\mathcal{N}(J_H^T(q_0, \Theta_0))) \leq 2$. Note that one dimension of $\mathcal{N}(J_H^T)$ lies in $\mathcal{N}(G)$, and represents the squeezing forces along the axis of the closing actuator. This 1-dimensional space either consists of active internal forces when the closing actuator displaces, or it is a space of preloading forces when the actuator is locked. When the two finger geometries are symmetric about a line passing through the grasped object (e.g., when the hand grasps a circle), $dim(U_{sd}) = 0$.

Proposition 3. *In a rigid body model of a two-fingered fractal hand, $dim(U_{act} = 0)$, while $dim(U_{sd}) \in \{0, 1\}$. When the closing actuator moves, $dim(N_{act}) = 1$ and $dim(N_{pre}) = 0$. Else $dim(N_{act}) = 0$ and $dim(N_{pre}) = 1$.*

Unfortunately, since $dim(U_{sd}) < 3$, our analysis shows that a 1^{st}-order rigid-body analysis (involving wrenches, velocities and point contacts) cannot fully explain the Fractal Hand's empirical ability to securely hold planar objects under arbitrary bounded perturbations: its observed ability to securely hold an object in equilibrium, even though the finger joints have no actuators, cannot be ascribed to structurally dependent contact forces. The next section provide one explanation for the fractal hand's behavior.

V. Perturbed Object Motion in a Fractal Hand

An equilibrium grasp of a 2-fingered fractal hand has the following useful property.

Proposition 4. *Consider a 2-fingered frictionless contact fractal hand that grasps a rigid object, $\mathcal{O}$, in an equilibrium grasp, q_0. When object $\mathcal{O}$ is perturbed infinitesimally by small amount $\dot{q}$ from equilibrium, the fractal finger joints, θ_1 and θ_2 are instantaneously motionless.*

Proof: When $\mathcal{O}$ is infinitesimally perturbed from its equilibrium configuration by $\dot{q}$, the set of object-side contact frames which contact the i^{th} finger move with velocities

$$V_{C_i^{\mathcal{O}}} = T_{OC_i^{\mathcal{O}}}^{-1}\dot{q}. \quad (10)$$

where matrix $T_{OC_i^{\mathcal{O}}}^{-1}$ transforms the object velocity to the $2^{(n-1)}$ contact frame velocities.

The corresponding finger-side contact frames move with the velocities transmitted across the contact normals:

$$V_{C_i} = \tilde{W}_i^T T_{\mathcal{C}_i C_i^{\mathcal{O}}} V_{C_i^{\mathcal{O}}} \quad (11)$$

where matrix $T_{\mathcal{C}_i C_i^{\mathcal{O}}}$ transforms the velocities of the contacts frames on the grasped object to the finger contact frames' coordinates.

Note that at a frictionless contact equilibrium grasp, the fingertip frame and finger-side contact frame will be identical. Hence, the admissible finger contact frame velocities can be related to each finger's joint velocities as:

$$V_{C_i} = J_{F,i}(\theta_{i,0})\dot{\theta}_i. \quad (12)$$

Combining the above equations yields the relationship:

$$J_{F,i}(\theta_{i,0})\dot{\theta}_i = \tilde{W}^T T_{\mathcal{C}_i C_i^{\mathcal{O}}} T_{OC_j^{\mathcal{O}}}^{-1}\dot{q}. \quad (13)$$

The joint velocities $\dot{\theta}_i$ that satisfy Eq. (13) are the possible mechanism joint movement responses to the perturbations in $\mathcal{O}$'s displacement. The set of all possible solutions to (13) consists of

$$\dot{\theta}_i = J_{F,i}^{\dagger}(\theta_{i,0})(\tilde{W}_i^T T_{\mathcal{C}_i C_i^{\mathcal{O}}} T_{OC_i^{\mathcal{O}}}^{-1}\dot{q}) + \dot{\theta}_{\mathcal{N},i} \quad (14)$$

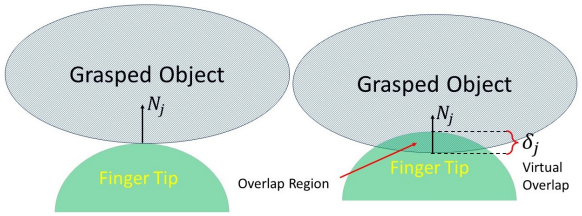

Fig. 6: Diagram of overlap model: a lumped parameter model of the interaction between a fingertip and the grasped object.

where $\dot{\theta}_{\mathcal{N},i}$ is any vector in the null space of $J_{F,i}(\theta_{i,0})$

Recall that $\mathcal{R}(J^{\dagger}_{F,i}) = \mathcal{R}(J^{T}_{F,i})$. We showed above that the matrix $J^{T}_{F,i}(\theta_{i,0})$ has a non-trivial null space in an equilibrium grasp, and that vectors normal to the fingertip surfaces lie in $\mathcal{N}(J^{T}_{F,k})$ Thus, matrix $\tilde{W}^{T}_{i}$ projects the velocities $T_{\mathcal{C}_i\mathcal{C}^{\mathcal{O}}_i} T^{-1}_{O\mathcal{C}^{\mathcal{O}}_i} \dot{q}$ onto $\mathcal{N}(J^{T}_{F,k})$ in the right hand side of Eq. (14). Thus, only internal joint motions, in $\mathcal{N}(J_{F,i})$ are possible solutions. These internal motions cause no movement of the fingertips. Hence, to 1^{st}-order, small perturbations of $\mathcal{O}$'s position yield no finger motions along the fingertip contact normals when the object lies in an equilibrium grasp. □

Thus, to understand the behavior of the grasped object under small perturbations in an equilibrium grasp, we must use a 2^{nd}-order motion analysis of the perturbed object. A future work will consider the 2^{nd}-order motion analysis that includes the velocities and acceleration of the finger mechanism joints. In this paper, the next section incorporates a compliance model, and the analysis of this section, to develop a preliminary result regarding fractal grasping security.

VI. Compliance Effects

This section introduces a lumped parameter model of object and finger tip compliance [11], [22]. This model will be combined with the results of previous section to provide our preliminary result on fractal grasps. Throughout this section, we assume frictionless contact between the fingertips and the object. For notational simplicity, we also drop the finger enumeration index $i \in \{1, 2\}$ when it is unnecessary.

A. Modeling Fingertip/Object Compliance

While the fingertips and object bodies may be stiff, their materials are elastically deformable in practice. As the object and a fingertip are pressed together, their surfaces will deform in proportion to the contact force magnitude. An *overlap* model [21], [22] captures compliance effects in a lumped parameter way, without using detailed surface deformation models. This approach assumes that the rigid fingertip and object shapes can virtually penetrate as the bodies are pressed together, with the net interaction force modeled as a function of the virtual overlap (Fig. 6).

Definition 5. [21], [22] The **overlap**, $\delta_j(\Theta, q)$, of the j^{th} fingertip with $\mathcal{O}$ is the minimum amount of translation needed to separate the undeformed fingertip body shape from the undeformed object body shape.

The Hertz contact model can be exactly captured by the contact force function $f_j = k\delta_j^{3/2}$ for a constant c that depends upon the bodies' geometry in the vicinity of the contact, and their material properties. The contact force model $f_j = k\delta_j$ is a good approximation of a linear spring compliance relationship. For more details, see [11], [26].

B. Fractal Finger Stiffness Matrix

A single finger's stiffness matrix can be derived from an expression for the potential energy, $\Pi(\cdot)$, due to the finger's deflection away from its equilibrium pose $(q_0, \Theta_{i,0})$ when the object and finger mechanism are perturbed from equilibrium:

$$\Pi(u) = \sum_{j=1}^{2^{n-1}} \int_{\delta_j(u_0)}^{\delta_j(u)} f_j(\delta_j) \cdot \frac{d\delta_j}{dt} dt = \sum_{j=1}^{2^{n-1}} \int_{\delta_j(u_0)}^{\delta_j(u)} f_j(\delta) \cdot d\delta_j \tag{15}$$

where the j^{th} contact force $f_j(\delta_j)$ arises from the compliant interaction between the j^{th} fingertip body and $\mathcal{O}$, and u is a notational simplification: $u = (q, \theta)^T$. Under the frictionless contact assumption, the scalar normal force f_j acts along the contact surface normal, N_j, and δ_j is the virtual overlap (see Fig. 6). The integrand of Eq. (15) is the power produced by the normal force acting through a differential displacement of the the contacting surfaces.

Assuming no finger mechanism losses (e.g., from joint friction) and no losses (e.g., heat dissipation) during material deformation, the integrals in Eq. (15) are independent of the specific paths followed by the fingertips. Hence, $\Pi(u)$ is conservative, and (15) can be evaluated using the rule:

$$\frac{d}{du} \int_{g(u)}^{h(u)} \vec{f}_j(\sigma_j) \cdot d\sigma_j \;=\; \vec{f}_j(h(u)) \cdot \frac{dh}{du}(u) - \vec{f}_j(g(u)) \cdot \frac{dg}{du}(u).$$

Using this rule, the gradient of $\Pi(q)$ takes the form:

$$\nabla_u \Pi(u) \;=\; \sum_{j=1}^{2^{n-1}} f_j(u) \nabla_u \delta_j(u). \tag{16}$$

The *Hessian* of $\Pi(u)$ at u_0 defines the finger stiffness matrix at an equilibrium grasp:

$$\nabla^2_u \Pi(u_0) = \sum_{j=1}^{2^{n-1}} \underbrace{\frac{df_j}{d\delta_j} \left(\nabla_u \delta_j \nabla_u \delta_j^T \right)}_{1^{st}-\text{order}, K^1} \Bigg|_{u_0} + \underbrace{f_j \nabla^2_u \delta_j}_{2^{nd}-\text{order}, K^2} \Bigg|_{u_0} \tag{17}$$

To analyze the equilibrium grasp, we assume hereafter that the closing actuator is locked at equlibrium. The potential energy, PE, of the compliant hand/object system for small (instantaneous) perturbations of both hand fingers and object takes the form: $PE = \dot{u}_1^T (K_1^1 + K_1^2) \dot{u}_1 + \dot{u}_2^T (K_2^1 + K_2^2) \dot{u}_2$ If PE is a positive definite function of $(\dot{q}\ \dot{\theta}_1\ \dot{\theta}_2)^T$, then the object/hand system is *locally compliantly stable.*

Remark: To analyze the security of $\mathcal{O}$, we are only concerned with the hand/object response to perturbations of $\mathcal{O}$. We use this response, which is provided by Prop. 4, to evaluate the definiteness of PE.

Proposition 6. *A two-fingered fractal equilibrium grasp of a non-exceptional planar object is compliantly stable to* 1^{st}*-order when* $n \geq 3$.

Proof: The first order stiffness term in Eq. (17) takes the form:

$$K_i^1 \triangleq \sum_{j=1}^{2^{n-1}} f_j^{'} \begin{bmatrix} \nabla_q \delta_j \nabla_q \delta_j^T & \nabla_q \delta_j \nabla_{\theta_i} \delta_j^T \\ \left(\nabla_q \delta_j \nabla_{\theta_i} \delta_j^T\right)^T & \nabla_{\theta_i} \delta_j \nabla_{\theta_i} \delta_j^T \end{bmatrix} \Big|_{u_0} \quad (18)$$

Using Proposition 4, the quadratic form $u^T(K_1^1+K_2^1)u$ takes the form

$$u^T(K_1^1 + K_2^1)u = \dot{q}^T\big(\sum_{i=1}^{2}\sum_{j=1}^{2^{n-1}} f_{i,j}^{'} \nabla_q \delta_{i,j} \nabla_q \delta_{i,j}^T|_{u_0}\big)\dot{q}.$$

Because this equilibrium grasp has more than 4 springy contacts arranged in a non-exceptional pattern (the contacts do not lie on a circle, parallel faces, or on opposite sides of an annulus), and noting that $f_j^{'} = df_j/d\delta_j$, is always a positive number for a hardening spring model, the 1^{st}-order stiffness matrix is positive definite [22]. □

Since the 1^{st}-order stiffness term is positive-definite, to estabilish stability of the grasped object, We need only show that the 2^{nd}-order stiffness contributions, K_1^2 and K_2^2, do not destabilize the 1^{st}-order term. The 2^{nd}-order contributions to the potential energy take the form:

$$u^T(K_1^2 + K_2^2)u = \dot{q}^T\big(\sum_{i=1}^{2}\sum_{j=1}^{2^{n-1}} f_{i,j} \nabla_q^2 \delta_{i,j}|_{u_0}\big)\dot{q}.$$

where, for a frictionless fingertip contact model, $\nabla_q^2 \delta_j$ take the form [11]:

$$\nabla_q^2 \delta_{i,j} = \frac{1}{r_F + r_{o_{i,j}}} \begin{pmatrix} \vec{n}_{i,j}\vec{n}_{i,j}^T - I & (r_{O_{i,j}} - \rho_{i,j})M\vec{n}_{i,j} \\ (r_{\mathcal{O}_{i,j}} - \rho_{i,j})(M\vec{n}_{i,j})^T & (r_F + \rho_{i,j})(r_{O_{i,j}} - \rho_{i,j}) \end{pmatrix}$$

where $\vec{n}_{i,j}$ is the unit vector normal to the boundary at the j^{th} contact with finger i. Scalars $r_{\mathcal{O}_{i,j}}$ and r_F respectively are the radii of curvature of the object and finger tip at their contact, while $\rho_{i,j} = \vec{n}_{i,j} \cdot \vec{p}_{i,j}$ and $\vec{p}_{i,j}$ is the vector from the origin of frame O to the j^{th} contact point in finger i. Matrix M was defined in Eq. (2).

At first glance, the 2^{nd}-order stiffness terms seem hard to analyze, and very problem dependent. However, note that for most practical designs, it is very difficult for the second order terms to be destabilizing. First, note $f_{i,j}^{'} >> f_{i,j}$ for most engineering materials, so that the 1^{st}-order terms stiffness terms are multiplied by a much large coefficient. Second, if the finger-tip radii of curvature is relatively flat, then $r_F >> 1$, and thus $1/(r_F + r_{O_{i,j}}) << 1$. Thus, modest constraints on the design of the fractal hand can ensure that nearly every non-exceptional equilibrium fractal hand grasp is compliantly stable.

VII. Conclusion

This paper and its companion introduced the fractal family of non-anthropomorphic robotic grippers, inspired by an obscure century-old mechanical vise. We formulated the routine kinematic description of this mechanism. More importantly, we showed that this single-actuator gripper has a remarkable property: every equilibrium grasp is compliantly stable, under mild finger design constraints. It is thus a significant extension of the widely-used parallel-jaw gripper. It also represents a novel line of synergistic robot hands– the fingers naturally and stably conform to essentially all object shapes. Because of these properties, planning for planar fractal grasps should be computationally simple. Future analytical work will investigate how the fingers' dimensions effect the quality of grasp security. The methods of analysis used in this paper are purely kinematic. Additional work needs to consider higher-order perturbations and dynamic effects in fractal grasps to ensure that these effects do not destroy the appealing stability that was found in this paper.

The companion paper [33] introduces principles to expand the vise-like design studied here to a larger class of fractal mechanisms, and to design a fractal hand for a given range of grasping tasks. It also introduces hand prototypes whose fingers can be 3-D printed in a single step, experiments conducted with the hand, and an initial 3-D finger prototype.

VIII. Acknowledgements

This work was supported in part by a grant from the Center for Autonomous Systems and Technologies at the California Institute of Technolgy.

References

[1] S. Abondance, C.B. Teeple, and R.J. Wood. A dexterous soft robotic hand for delicate in-hand manipulation. *IEEE Trans. Robotics*, 5(4):5502 – 5509, July 2020.

[2] A. Bicchi, M. Gabiccini, and M. Santello. Modelling natural and artificial hands with synergies. *Philosoph. Trans. Royal Society, B: Biological Sciences*, 356(1581):3153–3161, 2011.

[3] J.W. Burdick and E. Rimon. Wrench resistant multi-finger hand mechanisms. In *Proc. IEEE Int. Conf. Robotics Automation*, pages 2030–2037, May 2016.

[4] Chen-Hua Chiu Mao-Cheng Hsu Yang Chen Tzu-Yang Pai Wei-Geng Peng Chih-Hsing Liu, Ta-Lun Chen and Yen-Pin Chiang. Optimal design of a soft robotic gripper for grasping unknown objects. *Soft Robotics*, 5(4), 2018.

[5] Cosimo Della Santina, Matteo Bianchi, Giuseppe Averta, Simone Ciotti, Visar Arapi, Simone Fani, Edoardo Battaglia, Manuel Giuseppe Catalano, Marco Santello, and Antonio Bicchi. Postural hand synergies during environmental constraint exploitation. *Frontiers in Neurorobotics*, 11, 2017.

[6] Aaron M. Dollar and Robert D. Howe. The highly adaptive sdm hand: Design and performance evaluation. *The International Journal of Robotics Research*, 29(5):585–597, 2010.

[7] Neda Hassanzadeh, Shramana Ghosh, Nina Robson, and Alba Perez-Gracia. Velocity fields and tangent bundles for in-hand manipulative synthesis. 06 2016.

[8] N. Hassenzadeh. *Kinematic Synthesis Strategies for the Design of Robotic Hands*. PhD thesis, Idaho State University, 2017.

[9] N. Hassenzadeh, R. Movassagh-Kaniki, and A. Perez-Garcia. Design of a dexterous hand for a multi-hand task. In V. Parenti-Castelli, , and W. Schiehlen, editors, *ROMANSY 21 - Robot Design, Dynamics and Control*, pages 251–258. Springer, Cham, 2016.

[10] P.K. Kunze. Device for obtaining intimate contact with, engaging, or clamping bodies of any shape. U.S. Patent 1,059,545, 1913.

[11] Q. Lin, J.W. Burdick, and E. Rimon. Computation and analysis of natural compliance in fixturing and grasping arrangements. *IEEE Trans. Robotics and Automation*, 20(4), Aug. 2004.

[12] C. Liu1, P. Maiolino1, and Z. You. A 3d printable gripper based on thick panel origami. *Frontiers in Robotics*, 8, Sept. 2021.

[13] J. Mahler, J. Liang, S. Niyaz, M. Laskey, R. Doan, X. Liu, J.A. Ojea, and K. Goldberg. Dex-net 2.0: Deep learning to plan robust grasps with synthetic point clouds and analytic grasp metrics. In *Proc. Robotics: Science and Systems*, 2017.

[14] J. Mahler, M. Mat, Xinyu Liu andAlbert Li, D. Gealy, and K. Goldberg. Dex-net3.0:computing robust vacuum suction grasp targets in point clouds using a new analytic model and deeplearning. In *Proc. IEEE Int. Conf. Robotics Automation*, May 2019.

[15] A. Makhal and A. Perez-Gracia. *Solvable Multi-Fingered Hands for Exact Kinematic Synthesis*, pages 139–147. Springer International Publishing, Cham, 2014.

[16] R. Movassasagh, N. Hassenzaden, A. Makhal, and A Perez-Gracia. Design of a multi-palm robotic hand for assembly tasks. In *ASME Int. Design Engineering Tech. Conf.*, Aug. 2016.

[17] R.M. Murray, Z. Li, and S.S. Sastry. *A Mathematical Introduction to Robotic Manipulation*. CRC Press, 1994.

[18] G. Palli, C. Melchiorri, G. Vassura2, U. Scarcia1, L. Moriello, G. Berselli, A. Cavallo andG. De Maria, C. Natale, S. Pirozzi, C. May, F. Ficuciello, and B. Siciliano. The dexmart hand: Mechatronic design and experimental evaluation of synergy-based control for human-like grasping. *Int. J. Robotics Research*, 33(5), 2014.

[19] T. Pang, H.J.T. Suh, L. Yang, and R.Tedrake. Global planning for contact-rich manipulation via local smoothing of quasi-dynamic contact models. *IEEE Trans. Robotics*, pages 1–21, Aug. 2023.

[20] Hand Tool Rescue. Rare antique fractal vise [restoration]. YouTube, https://www.youtube.com/watch?v=QBeOgGt$_oWU$, 2021.

[21] E. Rimon and J.W. Burdick. Mobility of bodies in contact. ii. how forces are generated by curvature effects. *IEEE Trans. Robotics and Automation*, 1998, volume=14, number = 5, pages = 709-717.

[22] R. Rimon and J.W. Burdick. *The Mechanics of Robotic Grasping*. Cambridge Univ. Press, 2019.

[23] J. Romero, T. Feix, C.H. Ek H. Kjellstr¨om, and D. Kragic. Extracting postural synergies for robotic grasping. *IEEE Trans. Robotics*, 29(6):342–1352, 2013.

[24] J.K. Salisbury and J.J. Craig. Articulated hands: Force control and kinematic issues. *Int. J. Robotics Research*, 1(1), Spring 1982.

[25] C.D. Santina, C. Piazza, G. Grioli, M. G. Catalano, and A. Bicchi. Toward dexterous manipulation with augmented adaptive synergies: The pisa/iit softhand 2. *IEEE Trans. Robotics*, 34(5):1141–1156, 2018.

[26] A. Shapiro, E. Rimon, and A. Ohev-Zion. On the mechanics of natural compliance in frictional contacts and its effect on grasp stiffness and stability. 32(4):425–445, July 2013.

[27] E. Simo-Serra, A. Perez-Garcia, , H. Moon, and N. Robson. Kinematic synthesis of multi-fingered robotic hands for finite and infinitesimal tasks. In J. Lenarcic and M. Husty, editors, *Latest Advances In Robot Kinematics*, pages 173–180. Springer, New York, NY, 2012.

[28] E. Simo-Serra and A. Perez-Gracia. Kinematic synthesis using tree topologies. *Mechanisms and Machine Theory*, 72:94–113, 2014.

[29] Hannah Stuart, Shiquan Wang, Oussama Khatib, and Mark R Cutkosky. The ocean one hands: An adaptive design for robust marine manipulation. *Int. J. Robotics Research*, 36(2):150–166, 2017.

[30] Ali Tamimi and Alba Perez Gracia. Enumeration, structural and dimensional synthesis of robotic hands: theory and implementation. *ArXiv*, abs/1812.06348, 2018.

[31] Yusuke Tanaka, Yuki Shirai, Zachary Lacey, Xuan Lin, Jane Liu, and Dennis W. Hong. An under-actuated whippletree mechanism gripper based on multi-objective design optimization with auto-tuned weights. *IEEE/RSJ Int. Conf. Intelligent Robots and Systems*, pages 6139–6146, 2021.

[32] Adam Savage Tested. Adam savage in awe of this fractal vise! YouTube, https://www.youtube.com/watch?v=NUhrF0xkhhc, July 2023.

[33] M. Tisdale and J.W. Burdick. The Fractal Hand–II: Reviving a classic mechanism for contemporary grasping challenges. *(submitted) 2024 IEEE Int. Conf. Robotics and Automation. Aso available as ArXiv*, 2023.

[34] W. Yuan, S. Dong, and E.H. Adelson. Gelsight: High-resolution robot tactile sensors for estimating geometry and force. *Sensors*, 17(12), 2017.